

Nonlinear Photonic Crystals as a Source of Entangled Photons

Michiel J. A. de Dood,^{1,*} William T. M. Irvine,^{1,2} and Dirk Bouwmeester¹

¹*Department of Physics, University of California–Santa Barbara, Santa Barbara, California 93106, USA*

²*Department of Physics, University of Oxford, Parks Road, Oxford OX1 3PU, United Kingdom*

(Received 3 February 2004; published 22 July 2004)

Nonlinear photonic crystals can be used to provide phase matching for frequency conversion in optically isotropic materials. The phase-matching mechanism proposed here is a combination of form birefringence and phase velocity dispersion in a periodic structure. Since the phase matching relies on the geometry of the photonic crystal, it becomes possible to use highly nonlinear materials. This is illustrated considering a one-dimensional periodic $\text{Al}_{0.4}\text{Ga}_{0.6}\text{As}$ /air structure for the generation of $1.5\ \mu\text{m}$ light. We show that phase-matching conditions used in schemes to create entangled photon pairs can be achieved in photonic crystals.

DOI: 10.1103/PhysRevLett.93.040504

PACS numbers: 03.67.Mn, 42.65.Lm, 42.70.Qs

Polarization entangled photon pairs play a central role in testing the foundations of quantum mechanics and in implementing quantum information protocols [1]. They are likely to remain an appealing resource for practical quantum information science since they interact very little with the environment, propagate easily over long distances, and since photon polarization is easily manipulated in experiments. A popular method to create such pairs is by down-conversion in nonlinear crystals. For this process to be efficient the down-converted photons generated by pump photons at different points in the crystal have to be in phase with each other. This leads to the “phase-matching” condition $\vec{k}_p = \vec{k}_1 + \vec{k}_2$, for the wave vectors of the pump (\vec{k}_p) and down-converted photons (\vec{k}_1, \vec{k}_2). In general this condition will not hold owing to normal index dispersion which makes $|\vec{k}_p| > |\vec{k}_1| + |\vec{k}_2|$. The current schemes for down-conversion employ the natural birefringence of specific nonlinear crystals, like β -barium-borate (BBO), to compensate for this effect.

In one of these schemes [2,3], down-converted photons emerging in a particular pair of directions are entangled in polarization:

$$|\Psi\rangle = \frac{1}{\sqrt{2}}(|V\rangle_1|H\rangle_2 + e^{i\theta}|H\rangle_1|V\rangle_2), \quad (1)$$

where V and H denote the polarization state of particles 1 and 2 and θ is a phase factor that can be set by passing one of the photons through a phase plate.

Although birefringent nonlinear crystals have proven to be a successful source in many proof of principle experiments the demands of both practical quantum information and schemes for the implementation of all optical quantum computing [4] make it desirable to produce sources that are both more efficient and more easily integrable on, for example, an optical chip. The requirement that both the birefringence and the $\chi^{(2)}$ nonlinearity be naturally present severely limits the possibilities for improvement of sources based on existing crystals.

Semiconductors such as GaAs or GaP have a $\chi^{(2)}$, typically $200\ \text{pm/V}$ [5], about 2 orders of magnitude larger than that of commonly used crystals such as BBO, $2.2\ \text{pm/V}$ [6]. This, together with the existence of well developed microfabrication techniques for these materials, makes it attractive to explore ways of creating semiconductor based entangled photon sources. In these materials, which have no natural birefringence, the conditions for phase matching must be created artificially. In this Letter we show how photonic crystals can be used to achieve this.

Photonic crystals are materials with a periodic variation in refractive index on the scale of the optical wavelength. In layered structures the different boundary conditions at the interfaces for the two polarizations leads to an effective or “form” birefringence. The application of this effect to phase matching has been explored in the limit that the optical wavelength is much larger than the periodicity [7–9]. When the wavelength is comparable to the periodicity it was suggested that a reciprocal lattice vector can be added to the phase-matching conditions [10]. Alternatively a similar relation was found for periodically poled structures that have a periodicity in $\chi^{(2)}$, leading to quasi-phase-matching conditions [11]. Our work proposes how a combination of form birefringence and the strongly altered phase velocity in a photonic crystal can be used to phase match down-converted light and generate entangled photons.

We focus on one-dimensional structures for the sake of simplicity, although the concepts can be extended to two- and three-dimensional photonic crystals. The periodic variation in refractive index leads to Bragg scattering of the light, and wave propagation becomes best described in terms of a photonic band structure. If the wavelength is comparable to the periodicity of the structure, the propagation of light is strongly affected, leading to the existence of a range of frequencies, known as a stop band, for which light does not propagate.

The propagation of electromagnetic waves in a photonic crystal is described by Maxwell’s equations with a

periodic dielectric function $\epsilon(\vec{r})$. The general solution is given in terms of Bloch waves labeled by a frequency ω and a Bloch-wave vector \vec{K} and consists of a plane wave multiplied by a function that has the periodicity of the photonic lattice. The Bloch wave can be written as a Fourier sum over the reciprocal lattice vectors \vec{G} :

$$\vec{E}_{\vec{K}}(\vec{r}, t) = e^{-i(\vec{K}\cdot\vec{r}-\omega t)} \sum_{\vec{G}} \vec{e}_{\vec{K},\vec{G}} e^{-i\vec{G}\cdot\vec{r}}, \quad (2)$$

where $\vec{e}_{\vec{K},\vec{G}}$ are the Fourier coefficients for each of the space harmonics. For a one-dimensional structure \vec{K} and the coefficients $\vec{e}_{\vec{K},\vec{G}}$ can be obtained by finding the eigenvalues of a 2×2 transfer matrix for each polarization separately [6]. The effect of index dispersion, essential in any discussion of phase matching, can be easily incorporated as the transfer matrix is defined at each frequency separately. The obtained wave vector can be decomposed in components K_z perpendicular and k_{\parallel} parallel to the layers of the photonic crystal. The dispersion relation for transverse electric (TE) or ordinary (o) polarized waves, which have the electrical field in the plane of the layers, is given by [6]

$$K_z(\omega, k_{\parallel}) = \frac{1}{\Lambda} \arccos \left[\cos(k_{1z}a + k_{2z}b) - \frac{1}{2} \frac{(k_{1z} + k_{2z})^2}{k_{1z}k_{2z}} \sin(k_{1z}a) \sin(k_{2z}b) \right], \quad (3)$$

where k_{1z} and k_{2z} are the plane wave vector components perpendicular to the interfaces in medium one (of refractive index n_1) and medium two (of refractive index n_2):

$$k_{1,2z} = \sqrt{\left(\frac{n_{1,2}\omega}{c} \right)^2 - k_{\parallel}^2}.$$

An analogous expression can be derived for the orthogonal transverse magnetic (TM) or extraordinary (e) polarization, which results in different propagation constants. This important polarization dependence arises from the different boundary conditions at the interfaces for the two polarizations and plays a key role in the generation of polarization entangled photon pairs.

Figure 1 shows a band structure derived from Eq. (3) for a periodic structure with alternating layers of $\text{Al}_{0.4}\text{Ga}_{0.6}\text{As}$ and air. The fill fraction of $\text{Al}_{0.4}\text{Ga}_{0.6}\text{As}$ is 0.656. The gray area corresponds to propagating solutions for TM waves (left panel, negative k_{\parallel}) and TE waves (right panel, positive k_{\parallel}). They coincide for normal incidence ($k_{\parallel} = 0$). The solid lines in the figure correspond to light in vacuum ($\omega = c|\vec{k}|$) and divide the modes in those accessible to waves from outside the crystal, and those that are confined by total internal reflection. The latter modes can be accessed from the side of a sample or by using a set of prisms [12].

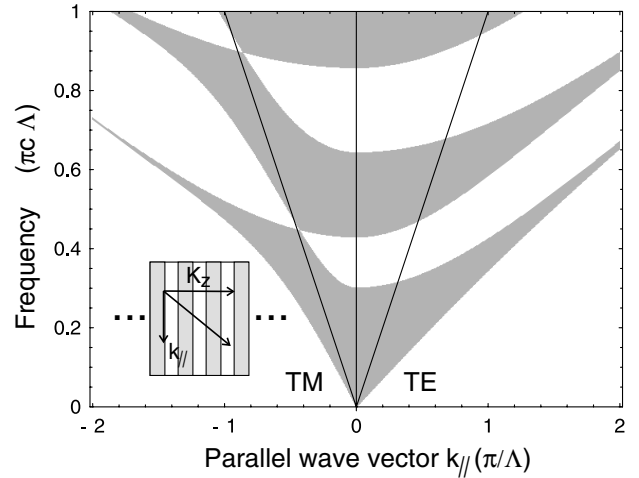


FIG. 1. Band structure of a periodic structure with $\text{Al}_{0.4}\text{Ga}_{0.6}\text{As}$ and air layers for TM (left) and TE (right) polarized light. The gray area corresponds to propagating solutions at a given frequency ω and wave vector k_{\parallel} . The solid lines indicate the “light line” in vacuum: $\omega = c|\vec{k}|$.

The frequency is specified in multiples of $\pi c/\Lambda$, where Λ is the periodicity of the structure. The structures were designed by first considering the refractive index to be equal to that at the pump frequency ω_p ($n = 3.4$ at $\lambda = 750$ nm). This allows the selection of a periodicity Λ such that the pump photons propagate in the structure. Once the periodicity is fixed, the frequency dependent refractive index is used to calculate dispersion surfaces to search for phase-matching conditions at relevant frequencies. The choice of material is motivated by the large second order nonlinearity together with the fact that it is transparent at a pump wavelength of 750 nm, to allow degenerate down-conversion in the important telecommunication window around 1500 nm. Moreover, the fabrication of such crystals seems to be feasible by starting with a periodic structure that has layers of AlAs and $\text{Al}_{0.4}\text{Ga}_{0.6}\text{As}$ followed by selective wet etching of the AlAs [13]. The fill fraction was chosen in order to maximize birefringence in the long wavelength limit ($\Lambda \ll \lambda$), where the Bloch waves are plane waves and experience an effective medium that behaves as a uniaxial birefringent material.

The leading terms in the Bloch-wave expansion in Eq. (2) will phase match when $\vec{K}_p + \vec{G}_p = \vec{K}_1 + \vec{G}_1 + \vec{K}_2 + \vec{G}_2$ where the \vec{G} s correspond to the leading $\vec{e}_{\vec{K},\vec{G}}$ s, ensuring efficient down-conversion into these modes. Two regimes are explored that lead to the generation of entangled photon pairs. We first discuss the long wavelength limit ($\Lambda \ll \lambda$) followed by the case where $\Lambda \sim \lambda$.

Figure 2 shows dispersion surfaces in the long wavelength limit for a structure with periodicity $\Lambda = 18.75$ nm and a pump wavelength of 750 nm ($0.05 \pi c/\Lambda$). One set of dispersion surfaces for the down-converted light, at 1500 nm wavelength, is drawn at the

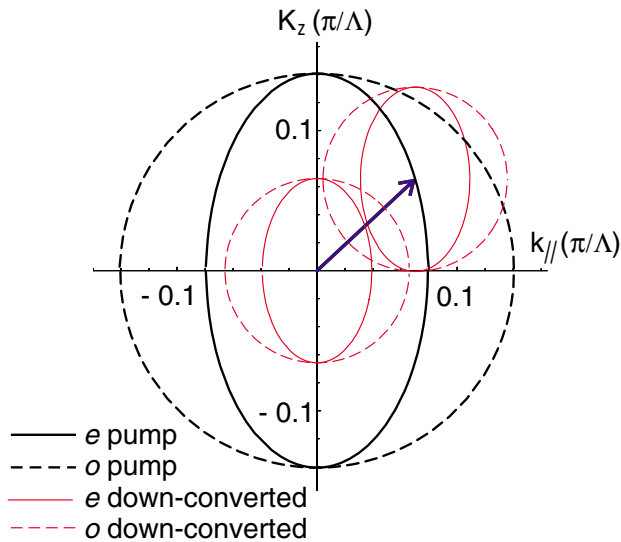


FIG. 2 (color online). Dispersion surfaces for degenerate down-conversion at 1500 nm in a one-dimensional $\text{Al}_{0.4}\text{Ga}_{0.6}\text{As}$ /air photonic crystal with a periodicity $\Lambda = 18.75$ nm and a fill fraction of $\text{Al}_{0.4}\text{Ga}_{0.6}\text{As}$ of 65.6%. Dispersion surfaces are shown for the pump at a wavelength of 750 nm (thick lines) and for degenerate down-conversion at 1500 nm (thin lines). The dashed lines correspond to TE (ordinary) polarization, while the solid lines correspond to TM (extraordinary) polarization. The pump wave vector indicated by the arrow is extraordinary.

origin; another is drawn at the end of the pump wave vector in order to obtain a simple geometric construction of the phase-matching condition. Wave vectors satisfying the phase-matching condition correspond, in such a diagram, to the intersections between the dispersion surfaces of the down-converted photons.

The intersections of the thin dotted lines represent the wave vectors of two ordinary (o) polarized photons, created by the extraordinary (e) polarized pump field. This situation is usually referred to as noncolinear type-I down-conversion. Since the structure is symmetric under rotations about the optical axis parallel to K_z , the circles and ellipses in Fig. 2 should be seen as spheres and ellipsoids. The intersections of the two down-conversion spheres for o polarization give a circle, representing a cone of down-converted light centered on the pump wave vector. Every pair of photons is emitted in such a way that they obey the phase-matching condition and so are always diametrically opposite each other about the pump.

For noncolinear type-II down-conversion, the pump field is e polarized and the down-converted photon pairs each have one o polarized and one e polarized photon. This case corresponds to the intersections of the dashed thin lines with the solid thin lines in Fig. 2. There are two pairs of such intersections, each representing an intersection between a sphere and an ellipsoid. They define two slightly distorted cones of down-converted light whose central axes are not aligned. For the direct generation of

polarization entangled photons as in Eq. (1), the e and o photons in a pair must be emitted in directions in which e photons and o photons are indistinguishable except by their polarization. This happens at the intersections of the two distorted cones discussed above.

Figure 3 shows dispersion surfaces for a photonic crystal with a periodicity $\Lambda = 187.5$ nm, a factor of 10 greater than that of Fig. 2 and comparable to the wavelength of the pump light. The frequency of the pump $\omega = 0.5\pi c/\Lambda$ ($\lambda = 750$ nm) is now above the first stop band for normal incidence. The dispersion surfaces for the pump are no longer continuous as some directions are excluded by Bragg reflection.

For the down-converted photons at a wavelength of 1500 nm, the Bloch waves are essentially plane waves with wave vectors \vec{K}_1 and \vec{K}_2 . The phase-matching condition in this case reduces to $\vec{K}_p + \vec{G}_p = \vec{K}_1 + \vec{K}_2$. The pump wave vector, indicated by the arrow, is chosen to end in the second Brillouin zone in order to select the reciprocal lattice vector that corresponds to the dominant space harmonic of the Bloch wave in Eq. (2). In principle, phase matching can also be achieved by choosing another reciprocal lattice vector, but the amplitude of the down-converted light will be reduced.

The dispersion surfaces of down-converted photons in Fig. 3 indicated by the thin lines resemble those of the long wavelength limit. Again there are two different types of intersections, corresponding to type-I ($e \rightarrow oo$) and type-II ($e \rightarrow eo$) down-conversion. As discussed in the long wavelength limit, polarization entangled

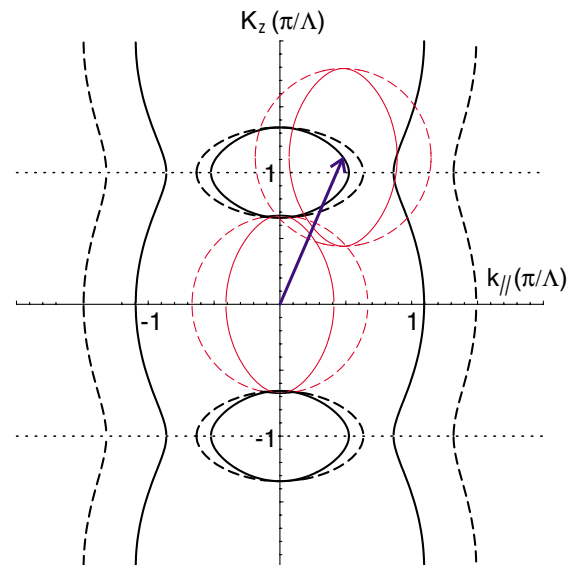


FIG. 3 (color online). Dispersion diagram in the repeated zone scheme for a pump wavelength of 750 nm. The periodicity of the crystal is $\Lambda = 187.5$ nm and the fill fraction of $\text{Al}_{0.4}\text{Ga}_{0.6}\text{As}$ is $\alpha = 0.656$. The pump wave vector is indicated by the arrow.

photons may be collected at the intersections of the distorted cones.

In the long wavelength limit the phase matching relies solely on form birefringence. However, when the periodicity of the crystal is comparable to the wavelength of the pump, the phase matching also relies on a substantial change in phase velocity. For frequencies below the stop band the phase velocity is lower than that in the long wavelength limit, which works against phase matching since it adds to the effect of normal index dispersion. However, if the frequency is above the frequency of the stop band the phase velocity is increased and compensates the effect of index dispersion. For large enough index contrast this can be used to achieve phase matching where all photons have the same polarization, i.e., $e \rightarrow ee$ or $o \rightarrow oo$.

We now estimate the efficiency of our scheme compared to that of the scheme based on BBO. There are four factors that contribute to the relative amplitude: (i) the ratio of the value of the $\chi^{(2)}$'s. (ii) The efficiency per unit length should be multiplied by the fill fraction of $\chi^{(2)}$ material (0.65). (iii) The scheme phase matches the leading term of the Bloch waves. The magnitude of this term is obtained by Fourier analysis of the Bloch wave. This gives a factor of ~ 1 and a factor ~ 0.21 for the structures in Figs. 2 and 3, respectively. (iv) As for any nonlinear material we need to consider the tensor properties of the nonlinearity. $\text{Al}_{0.4}\text{Ga}_{0.6}\text{As}$ has the $\bar{4}3m$ point group symmetry and for the conventional (100) surface orientation and our directions this gives a factor of ~ 0.83 and ~ 0.53 . Multiplying all factors and squaring to get the relative efficiency gives ~ 2500 and ~ 50 times the efficiency for BBO.

The example structures we used to illustrate our scheme have by no means been tailored to maximize the efficiency. The large value of $\chi^{(2)}$ in $\text{Al}_{0.4}\text{Ga}_{0.6}\text{As}$ leaves ample room for tailoring the geometry of the structure to suit a particular application, while keeping the process efficient. It should be noted that there is a trade-off between increasing the strength of the interaction of light with the photonic crystal and the loss in efficiency associated with the undesired terms in the Bloch-wave expansion (cf. the efficiency for Figs. 2 and 3). An interesting extension of our work is to consider down-conversion of pulsed Gaussian beams, which is accompanied by spatiotemporal walk-off effects that affect the quality of entanglement and the efficiency of the process. It seems promising to explore the difference between group velocity and phase velocity in a photonic crystal to reduce these effects.

The concepts introduced in this Letter can be extended to two- and three-dimensional photonic crystals. The change in phase velocity is a result of Bragg reflection common to all photonic crystals. Form birefringence relies on polarization dependent boundary conditions

and is observed in one- and two-dimensional photonic crystals. Form birefringence can be introduced in three-dimensional structures by making the individual scatterers elongated which can be achieved in microfabricated structures [14] or by deforming a colloidal crystal [15].

We presented a phase-matching scheme that uses the combined effects of form birefringence and a change in phase velocity in photonic crystals to enable the production of entangled photon pairs. Both effects can be tuned by designing an appropriate structure and are decoupled from the intrinsic nonlinearity that is determined by the choice of the constituent materials. We focused primarily on III-V semiconductors and on AlGaAs , in particular. These materials have a high nonlinearity together with a large linear refractive index which contribute to a strong interaction with light. Microfabrication techniques are well developed for these materials and an experimental realization seems feasible. If successful, the structure could be implemented on optical chips as an integrated source of entangled photons.

We are most grateful to Mark Sherwin and Evelyn Hu for stimulating discussions. W. I. acknowledges Elsas s.p.a. for support under MIUR Grant No. 67679/L.488/92. M. d. D and D. B. acknowledge support under DARPA Grant No. MDA972-01-1-0027.

*Corresponding author.

Electronic address: mdedood@physics.ucsb.edu

- [1] D. Bouwmeester, A. Ekert, and A. Zeilinger, *The Physics of Quantum Information* (Springer, Berlin, 2000), and references therein.
- [2] P. G. Kwiat, K. Mattle, H. Weinfurter, A. Zeilinger, A. V. Sergienko, and Y. Shih, *Phys. Rev. Lett.* **75**, 4337 (1995).
- [3] C. Kurtsiefer, M. Oberparleiter, and H. Weinfurter, *J. Mod. Opt.* **48**, 1997 (2001).
- [4] E. Knill, R. Laflamme, and G. J. Milburn, *Nature (London)* **409**, 46 (2001).
- [5] S. Bergfeld and W. Daum, *Phys. Rev. Lett.* **90**, 036801 (2003).
- [6] A. Yariv and P. Yeh, *Optical Waves in Crystals* (Wiley, New York, 1976).
- [7] J. P. van der Ziel, M. Ilegems, and R. M. Mikulyak, *Appl. Phys. Lett.* **28**, 735 (1976).
- [8] A. Fiore, V. Berger, E. Rosencher, P. Bravetti, and xsJ. Nagle, *Nature (London)* **391**, 463 (1998).
- [9] A. De Rossi, V. Berger, M. Calligaro, G. Leo, V. Ortiz, and X. Marcadet, *Appl. Phys. Lett.* **79**, 3758 (2001).
- [10] K. Sakoda and K. Ohtaka, *Phys. Rev. B* **54**, 5742 (1996).
- [11] V. Berger, *Phys. Rev. Lett.* **81**, 4136 (1998).
- [12] P. K. Tien, R. Ulrich, and R. J. Martin, *Appl. Phys. Lett.* **14**, 291 (1969).
- [13] E. Yablonovitch, T. Gmitter, J. P. Harbison, and R. Bhat, *Appl. Phys. Lett.* **51**, 2222 (1987).
- [14] S. Y. Lin *et al.*, *Nature (London)* **394**, 251 (1998).
- [15] K. P. Velikov, T. van Dillen, A. Polman, and A. van Blaaderen, *Appl. Phys. Lett.* **81**, 838 (2002).